Applied Clay Science 88–89 (2014) 100–110

Contents lists available at ScienceDirect

Applied Clay Science

journal homepage: www.elsevier.com/locate/clay

Research paper

Assessment of two clayey materials from northwest Sardinia (Alghero district, Italy) with a view to their extraction and use in traditional brick production

B. De Rosa [a], G. Cultrone [b,*]

[a] Dipartimento di Scienza della Natura e del Territorio, Università di Sassari, via Piandanna 4, 07100 Sassari, Italy
[b] Departamento de Mineralogía y Petrología, Facultad de Ciencias, Universidad de Granada, Avda. Fuentenueva s/n, 18002 Granada, Spain

ARTICLE INFO

Article history:
Received 24 December 2012
Received in revised form 8 November 2013
Accepted 21 November 2013
Available online 21 December 2013

Keywords:
Raw materials
Fired ceramics
Petrophysical properties
Durability

ABSTRACT

Two clayey raw materials collected in the Porto Ferro and Lago Baratz areas of Alghero in northwest Sardinia (Italy) were used to prepare handmade brick samples that were fired under oxidizing conditions at temperatures ranging between 750 and 1000 °C to evaluate their possible use in the brickmaking industry. Both raw materials are rich in quartz and phyllosilicates but only the sample from Porto Ferro contains calcite. Granulometrically, the sample from Porto Ferro is a silty sand and shows higher plasticity than the clay from Lago Baratz which is classified as a sand. After firing, the samples acquire a red-orange colour and undergo significant mineralogical and textural changes. Phyllosilicate depletion is accompanied by the crystallisation of mullite and, only in Porto Ferro samples, the breakdown of calcite is followed by the formation of gehlenite, wollastonite and anorthite. Optical and electronic microscopic observations revealed that the temper grains are larger and more abundant in the bricks from Lago Baratz than in those from Porto Ferro. As firing temperature increased, pores became ellipsoidal in shape and the matrix became vitrified. The samples from Lago Baratz also show fissures at grain boundaries, which indicate the formation of an extensive network of pores and make these bricks very brittle when fired at low temperatures (750 and 800 °C), so much so that hydric tests could not be performed on them. Bricks produced with the clayey material from Porto Ferro achieved the best results in terms of hydric behaviour, with a reduction in the water absorption capacity, and in terms of compactness, with an increase in ultrasound wave velocity. However, both Porto Ferro and Lago Baratz bricks behaved in similar ways when submitted to the salt crystallisation test, especially at 1000 °C when a sufficient degree of vitrification was reached to ensure high quality samples.

1. Introduction

In ceramic manufacture, a raw material is mixed with water and moulded to give it the shape we want to produce; it is then dried and finally fired. Despite advances in technology the same basic procedure has been used for thousands of years. During this procedure various choices have to be made that have a direct effect on the final product. Two of these, the choice of the raw material and of the firing temperature, are of major importance, as the first affects the type of ceramic that can be produced, while the second influences the quality of the final product (Rathossi and Pontikes, 2010; Warren, 1999). Research has shown for example that the type of clay, the size and amount of temper and the presence of fluxing agents in a raw material will allow the production of a wide range of ceramics from a rough brick to the finest porcelain (Dondi and Fabbri, 2001; Singer and Singer, 1963). Similarly, different firing temperatures alter the mineralogy and the texture of the ceramics in different ways, making them more or less durable (Cultrone et al., 2001, 2004).

In this paper we analyse the granulometry and mineralogy of two clayey materials from northwest Sardinia (Italy). We also study the petrography and physical properties of bricks made with these materials in order to evaluate their durability and potential for use in the brickmaking industry. The idea of studying these raw materials emerged after an archaeological excavation of the Nuragic site of Sant'Imbenia (Porto Conte area, Alghero district, 14th–7th century B.C.) in which ceramic objects were discovered and analysed (De Rosa, 2010). Previous research suggests that these ceramics were produced in the area with locally sourced raw materials (De Rosa et al., 2012). These raw materials are not quarried today but, the petrography of the archaeological findings suggests that they are different from granulometric and mineralogical points of view. This means that the methods used here could also be used to assess the potential for use in brick production of other raw materials with similar characteristics.

There is ample evidence of ceramic production using local clays in this part of the island over a wide chronological period. It has been demonstrated that ceramic products formed part of the daily lives of the

* Corresponding author. Tel.: +34 958 240077; fax: +34 958 248535.
E-mail address: cultrone@ugr.es (G. Cultrone).

0169-1317/$ – see front matter © 2013 Elsevier B.V. All rights reserved.
http://dx.doi.org/10.1016/j.clay.2013.11.030

inhabitants of villages such as Sant'Imbenia, Barnaldu and Palmavera among others, from at least the Neolithic Age, if not earlier (Colombi, 2010; Moravetti, 1992). Recent studies have revealed the trade in Sardinian ceramics in the Mediterranean Basin during the first millennium B.C. (Fundoni, 2009; González de Canales Cerisola et al., 2006). Later on, the Romans manufactured ceramics in the Porto Conte area and in the Turris Libisonis colony along the sea coast near Porto Torres (Carboni et al., 2012). There is also evidence of ceramic production in the Alghero (Milanese, 2013) and Sassari areas (Rovina and Fiori, 2013) in the Middle Ages.

According to the data supplied by the Italian Association of Brick Manufacturers (ANDIL, http://www.laterizio.it/), Sardinia today has a low brick production level (229,702 tonnes in 2011, less than 3% of total national production) compared to other regions in Italy, one of Europe's biggest brick manufacturers (Dondi, 2011). There are only five registered factories in Sardinia out of 170 in the whole country, some of which are located in the south of the island where tertiary clay sediments are quarried (Strazzera et al., 1997). Another important production centre is the Campidano plain of Oristano in mid-western Sardinia where terracotta vessels, roof tiles and bricks are produced (Annis, 1985). Quarries in northern Sardinia typically contain Quaternary colluvial clays derived from silty–sandy–conglomeratic sediments (Dondi et al., 1999a). The most common bricks produced in the area are hollow bricks characterized by low porosity and pore size and low resistance to frost (Dondi et al., 1999b). Despite the fact that brick production on the island is currently low, several studies have highlighted the potential of northwest Sardinia for ceramic production (Ligas et al., 1997; Oggiano and Mameli, 2012).

Although most brick production today is performed by extrusion (Lassinantti Gualtieri et al., 2010; Sánchez, 2001), as is the case in Sardinian factories (Dondi et al., 1995), in this paper we will be considering traditional handmade brick manufacture. This is because of the demand from architects and builders for special, non-standard bricks (with varying sizes, shapes and finishes), which are generally used in the construction of traditional-style country houses and in the restoration of historical buildings (Bajare and Svinka, 2000; Trevelyan and Haslam, 2001; Warren, 1999). Handmade brick production has an additional advantage over industrially produced extruded bricks in that it offers greater flexibility in terms of the numbers of bricks produced, so enabling savings in raw materials (Trevelyan and Haslam, 2001).

There are various differences between traditional and extruded bricks: in traditional bricks more water is used during the moulding process, the preferred orientation of laminar minerals is less pronounced and, above all, the final product is more porous (Álvarez de Buergo Ballester and González Limón, 1994; Singer and Singer, 1963). This last aspect makes traditional bricks more prone to decay. Particular attention must therefore be paid to the tests measuring physical parameters such as the compactness, water absorption and durability of the fired bricks. However, lower physical parameters with respect to extruded bricks should not necessarily be seen as a synonym of defective or of low quality products. In fact, the hydric, porometric and mechanical parameters of handmade bricks often closely resemble those of bricks used in our Cultural Heritage (Esbert et al., 1997) and are therefore more compatible with them than extruded bricks. The use of compatible materials in restoration work is crucial to avoid further damage to the monuments (Elert et al., 2003). Although stone is the most commonly used material in Sardinia's historical monuments, there are some fine brick buildings in Siligo and Fertilia (Sassari district) and, of course, in mainland Italy. We therefore believe our results will be of interest to those working in the restoration and traditional construction sectors.

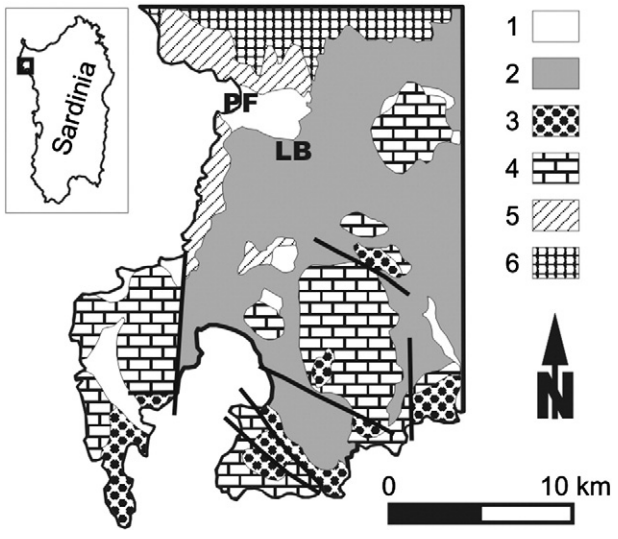

Fig. 1. Geological map of the area near Alghero (Sardinia, Italy) where the raw materials from Porto Ferro (PF) and Lago Baratz (LB) were collected. Legend: 1) alluvial, eolian and littoral sediments (Holocene); 2) conglomerates, sand and mud deposits in river terraces (Pleistocene); 3) limestones and marls of sub-littoral environment (Cretaceous); 4) dolomitic and bioclastic limestones and marls (Lias-Malm); 5) red-violet silty clays, micaceous and quartz-rich sandstones known as "Buntsandstein" (Upper Permian–Lower Triassic); and 6) Metasandstones and phyllites, terrigenous sedimentary rocks of uncertain age. Black lines indicate discontinuities. From Carmignani (2001), modified.

2. Materials and methods

2.1. Materials provenance and geology of the area

Two raw materials for ceramic production were collected from the Alghero district (northwest Sardinia) in the Porto Ferro (PF) and Lago Baratz (LB) areas.

The PF samples come from an area near the Bay of Porto Ferro (coordinates: 40°41′36.90″N; 8°11′56.72″E), a natural inlet about 2 km long, bordered to the south by twenty-metre high dunes that separate it from the Lago Baratz. The raw material is reddish-brown and very plastic. The LB was sampled near the only natural lake in Sardinia, the Lago Baratz (coordinates: 40°40′46.42″N; 8°13′38.06″E). It was formed at the end of the Würm Glaciation Stage and is characterized by significant seasonal variations in water levels (Alba, 2009). The raw material is almost brown and slightly plastic, with an earthy texture. The geology of the area consists mainly of Mesozoic layers, which rest on Quaternary deposits related to alluvial fans and/or flat braided channels, and wind dune fields from the Würm Glaciation Stage (Fig. 1) (Cassinis et al., 1996). The Triassic is mainly composed of dolostones and aeolian sandstones with carbonate cement, dolomitic marls, chalk marls and clay with foraminifera and continental facies, consisting of the typical red Buntsandstein sandstone. The Jurassic and the Cretaceous deposits consist of platform carbonates: mainly dolostones, limestones and marl. On the top, there are outcrops of volcano-sedimentary successions and lacustrine deposits from the early Oligocene–Miocene (Cita Sironi et al., 2006).

Geomorphologically, the study area is made up of level to sublevel land used above all for agriculture. Judging by the geographical extension of the outcrops from where the raw materials were sampled, both PF and LB reserves appear to be vast. Slightly further to the north, similar sediments with large reserves are used in the brickmaking industry and abandoned areas are reused in a sustainable way as controlled landfills (Dondi et al., 1995).

2.2. Sample preparation process

The samples were prepared manually, by disaggregating the raw materials and adding the amount of water needed to soften the clayey mass and remove excess air. The mass was then placed in a wooden prism-shaped mould which had previously been lined with sand to prevent the clay from sticking to the walls. The mould dimensions were 24.4 × 11.5 × 4 cm. After 4 days, the samples, still moist, were removed

from the moulds and cut into smaller cube-shaped samples, with edges about 3 cm long. Once dried, the samples were heated in an electric oven (Herotec CR-35) with a fixed heat source for 1 h at 100 °C to remove residual moisture, and then fired under oxidizing conditions in the same oven at 750, 800, 850, 900 and 1000 °C. One hour after the final temperature was reached, the oven was switched off. The samples were then left for 24 h in the switched-off oven, so that cooling could be gradual and slow. After removal from the oven, fired samples were immersed in water to prevent a possible "lime blowing" phenomenon (Laird and Worcester, 1956) due to the presence of residual carbonate grains after firing.

The samples studied in this work are identified using abbreviations (PF or LB) to indicate the source of the raw material (Porto Ferro or Lago Baratz), followed by the numbers 750, 800, 850, 900 or 1000, which refer to the firing temperature. When there are no numbers, this means that the analysis was performed on unfired raw materials.

2.3. Analytical techniques

The grain size distribution for the two raw materials was determined by a laser-beam particle size analyzer (Malvern Mastersizer 2000LF).

The mineralogy of the raw materials and the clay-size fraction (<2 μm) was studied by X-ray diffraction (XRD) using a Philips PW 1710 diffractometer with a graphite monocromator and automatic collimator. Working conditions were as follows: CuKα radiation emission ($\lambda = 1.5405$ Å), 40 kV voltage, 40 mA current, 3° to 60° 2θ explored area and 0.05° $2\theta s^{-1}$ goniometric speed. XRD goniometric calibration was performed using a silicon standard. We used the random crystalline powder method for the total sample and the oriented aggregate method for the <2 μm fraction. The clay-size fraction was separated from the total sample by centrifugation using a Kubota KS-8000 apparatus. Data interpretation was performed using the XPowder® software (Martín Ramos, 2004). We performed a quantitative analysis of mineral phases using non-linear least square methods to fit full-profile diffractograms and compared the results to the standard values in the database. The PDF2 database and Normalized RIR method were used to identify the mineral phases. No internal standard mineral was added to the samples. To better estimate the amount of the vitreous phase developed after firing, the quartz content was considered as constant (Huertas et al., 1991). Note that the results of the analysis of vitreous phase should be taken as an approximation; however, they are more reliable when analysing samples of similar composition (Martín Ramos, 2004) as in the case of PF and LB bricks. More details of this quantitative analysis process can be found in Chapter 6 of the XPowder® software user's guide (http://www.xpowder.com/).

Bulk chemical analyses of PF and LB were performed by means of the X-ray fluorescence (XRF) technique, using a S4 Pioneer (Bruker AXS) spectrometer. Five grammes per sample were finely ground and well mixed in an agate mortar before being pressed into an Al holder for disk preparation. The estimated detection limit for major elements was 0.01 wt.%. The ZAF correction was performed systematically (Scott and Love, 1983). The NCS DC 74301 (GSMS-1) standard (Chen and Wang, 1998) was applied.

Atterberg limits are basic parameters in the characterization of soils and they were used to establish the liquid and plastic limits and the plasticity index of the two raw materials on the basis of their water content following the ASTM D 4318-10 (2010) standard. The liquid limit (L_L) represents the water content at which a soil changes from plastic to liquid behaviour. The plastic limit (L_P) is the lowest water content at which cylindrical threads of 3 mm in diameter can be moulded without crumbling. Finally, the plasticity index (P_I) was determined as the difference between L_L and L_P and represents the range of water content in which the soil has a plastic consistency.

In addition, bricks fired between 750 and 1000 °C were studied taking into account their colour, mineralogy, texture and physical parameters in order to assess their technical quality. L*a*b* coordinates assessed in brick samples were measured using a portable Minolta CM700d spectrophotometer. The measurements were performed by selecting CIE illuminant D65, which simulates daylight with a temperature colour of 6504 K.

The mineralogy and possible development of new silicate phases through firing was studied using XRD with the same apparatus and working conditions described above for the raw materials.

The texture of the brick samples was observed in thin sections with a polarizing optical microscope (POM, Olympus BX60), while the microtexture and the composition of some phases were determined using a field emission scanning electron microscope (FESEM, Leo Gemini 1530) coupled with Oxford Inca 200 energy dispersive X-ray microanalysis (EDX). Images were acquired in back-scattered mode (BSE) using polished thin carbon-coated sections.

The parameters associated with fluid uptake and transport inside the pores were determined by free (A_b) and forced water absorption (A_f) (EN, 13755, 2008) and drying (Di) (Normal 29/88, 1988) as follows:

$$A_b = \frac{M_L - M_0}{M_0} \times 100,$$

$$A_f = \frac{M_S - M_0}{M_0} \times 100,$$

$$Di = \frac{\int_{t_0}^{t_f} f(M_t)dt}{M_S \times t_f},$$

where M_0 is the mass of the dried sample, M_L is the mass of the sample saturated with water at atmospheric pressure (until constant mass is reached), M_S is the mass of the sample saturated with water under vacuum, M_t represents a decreasing water weight content as a function of time and t_0 and t_f are respectively the start and end times for the test.

On the basis of these measurements, the saturation coefficient (S), the apparent (ρ_b) and real (skeletal) densities (ρ_{sk}), and the open porosity (p_o) (RILEM, 1980) were determined as follows:

$$S = \frac{M_{48h} - M_0}{M_S - M_0} \times 100,$$

$$\rho_b = \frac{M_0}{M_S - M_H},$$

$$\rho_{sk} = \frac{M_0}{M_0 - M_H},$$

$$p_o = \frac{M_S - M_0}{M_S - M_H} \times 100,$$

where M_{48h} is the mass of the sample after 48 h immersion in water at atmospheric pressure and M_H is the mass of the sample saturated with water under vacuum and weighed in water.

Ultrasound is an excellent technique for determining the physical properties of ceramics because of its non-destructive nature. Ultrasound measurements were performed using a Steinkamp ultrasound generator with 100 kHz transducers. The transducers had a diameter of 2.7 cm. A viscoelastic couplant was used to ensure good coupling between transducers and brick samples. The propagation velocity of ultrasonic pulses (V_P) was measured in accordance with the ASTM D 2845-08 standard (2008) on dry test samples. These data were used to obtain information on the degree of compactness of the bricks. The total (ΔM) and relative anisotropies (Δm) (Guydader and Denis, 1986) were calculated as follows:

$$\Delta M = \left(1 - \frac{2V_{P1}}{V_{P2} + V_{P3}}\right) \times 100,$$

$$\Delta M = \left(\frac{2(V_{P2} - V_{P3})}{V_{P2} + V_{P3}}\right) \times 100,$$

where V_{P1}, V_{P2} and V_{P3} are the velocities measured in three perpendicular directions.

Finally, in accordance with the EN 12370 standard (2001), 10 cycles of salt crystallisation were performed using a 14% $NaSO_4 \times 10H_2O$ solution, which can exert a crystallisation pressure in confined spaces of 14 MPa (Espinosa Marzal et al., 2011). This test provided information on the damaging effects of the soluble salts that are usually present in water and can crystallize in pores and fissures. Three samples per brick type were used. The damage produced by the salt crystallisation test was evaluated via visual inspection of material loss and weight changes.

3. Results and discussions

3.1. Raw materials

XRD analysis of the clayey samples showed that the PF material is rich in quartz, phyllosilicates (muscovite type), feldspar, low calcite with traces of hematite. The clay-size fraction consists of illite and lesser amounts of kaolinite (Fig. 2 and Table 1). The raw material collected in the area around Lago Baratz (LB) has a slightly higher amount of quartz, and almost the same quantities of phyllosilicates, feldspar and hematite contents as PF. One important difference, however, is that it does not contain any calcite. The clay minerals identified were the same as in PF, but in this case illite and kaolinite occur in similar concentrations (Fig. 2 and Table 1).

PF and LB are chemically similar, both being rich in SiO_2 (50 wt.% and 59 wt.%, respectively) due to the presence of quartz crystals as identified by XRD, and show almost the same concentration of Al_2O_3, Fe_2O_3 and K_2O. The biggest difference is in CaO content, which is greater in PF reflecting the presence of calcite.

Both raw materials show a bimodal particle-size distribution but the two curves in Fig. 3 are different in shape. In fact, PF has two peaks of almost the same concentrations at 20 and 400 μm. The LB sample is poorer in finer fractions with a maximum in particle size around 600 μm and a second smaller peak at 55 μm. This difference affects the size of the specific surface area, which is bigger in PF (0.769 m^2/g) than in LB (0.335 m^2/g). On the basis of the Shepard (1954) nomenclature, PF is classified as silty sand while LB is a sand. The two raw materials plotted on Winkler's (1954) diagram (not shown) suggest that PF and LB can be used for common brick production even if the addition of finer fractions is advisable in the manufacturing process. However, previous research has shown that the results of this empirical diagram cannot rule out the possibility of a particular raw material being suitable for use in the production of different types of ceramic (Khalfaoui and Hajjaji, 2010).

As regards to the Atterberg limits, PF shows higher liquid and plastic limits than LB (Table 1). PF can be defined as a soil of medium plasticity ($P_I = 21.14$), whereas that of LB is of low plasticity ($P_I = 8.80$). This clear difference is because the raw material from PF is richer in finer fractions than LB (Fig. 3) and also because of the higher concentration of illite compared to kaolinite in the PF soil (Table 1). In fact, of the various clay minerals, illite is characterized by higher liquid and plastic

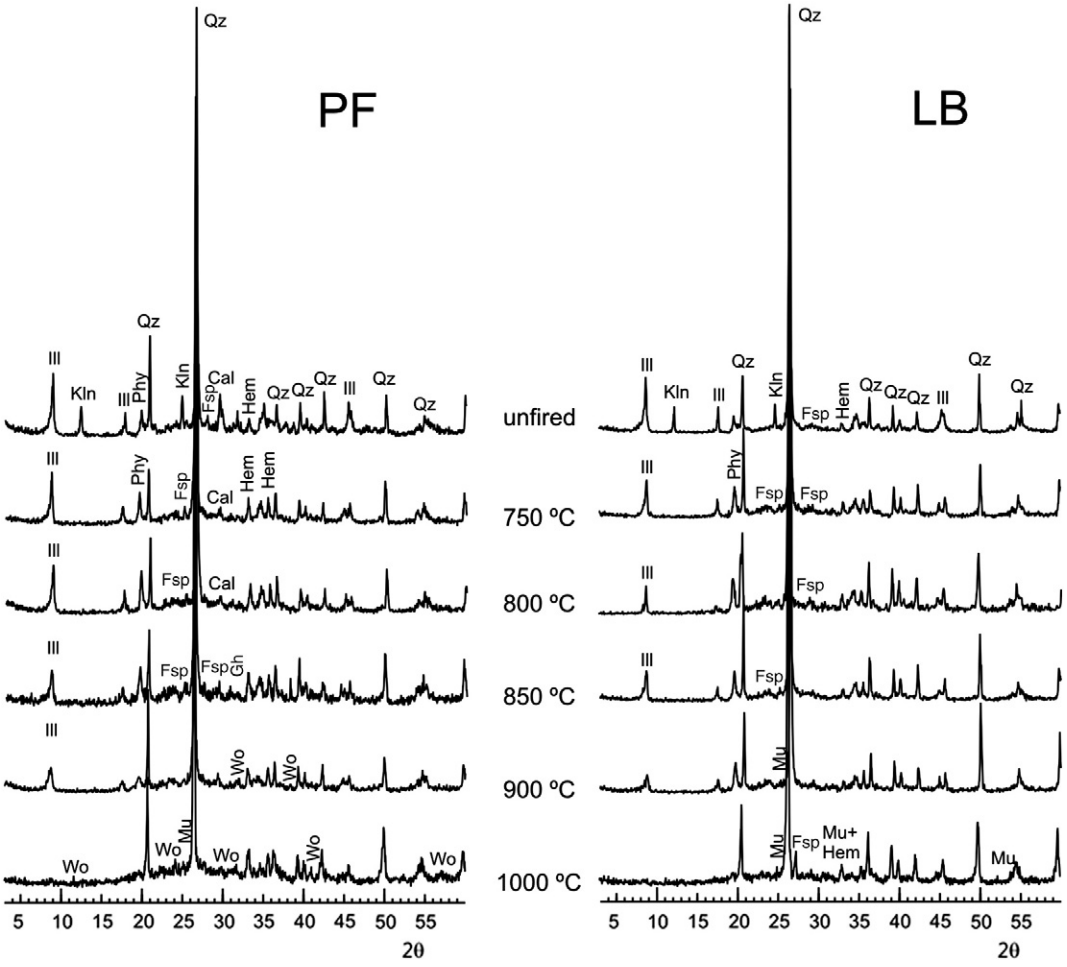

Fig. 2. Powder X-ray diffraction patterns of Porto Ferro (PF) and Lago Baratz samples (LB) as raw materials (unfired) and fired bricks at 750, 800, 850, 900 and 1000 °C. Legend: Qz = quartz; Ill = illite; Phy = phyllosilicates (in general); Cal = calcite; Hem = hematite; Fsp = feldspars (in general); Gh = gehlenite; Wo = wollastonite; and Mu = mullite. Mineral symbols after Whitney and Evans (2010).

Table 1
Mineralogical and chemical composition (in %) of the raw materials of Porto Ferro (PF) and Lago Baratz (LB) along with the Atterberg limits. L_L = liquid limit; L_P = plastic limit; P_I = plasticity index. Qz = quartz, Phy = phyllosilicates (in general), Fsp = feldspars (in general); Cal = calcite; Hem = hematite; Ill = illite; and Kln = kaolinite (mineral symbols after Whitney and Evans, 2010).

	Total sample					Clay fraction		Atterberg limits			
Sample	Qz	Phy	Fsp	Cal	Hem	Ill	Kln	L_L	L_P		P_I
PF	58	22	11	6	3	63	37	42.04	20.90		21.14
LB	65	19	14		2	55	45	25.75	16.95		8.80
	SiO_2	Al_2O_3	TiO_2	CaO	MgO	MnO	Na_2O	K_2O	Fe_2O_3	P_2O_5	L.O.I.
PF	50.33	20.73	0.74	4.65	1.43	0.02	1.15	5.00	6.26	0.06	9.61
LB	59.45	21.00	0.63	0.70	1.35	0.01	0.42	5.32	5.23	0.09	5.81

limits than kaolinite (Mitchell and Soga, 2005). Based on the clay workability chart (Bain and Highley, 1979), PF exhibits optimal moulding properties and is more suitable for use in producing bricks than pottery. LB falls outside but very close to the acceptable moulding properties field. The poor cohesion of this soil can be improved if it is blended with a soil of higher plasticity.

3.2. Fired products

Some preliminary results may already be drawn from the behaviour of the samples during the firing process. The PF samples responded best to all firing temperatures, with good compactness of the product once removed from the oven. The LB samples, on the other hand, showed good results only above 800 °C, while at lower temperatures (750 and 800 °C) they were brittle and not very hard. This poor behaviour at low temperatures is attributable to the coarse-grained fraction content and low plasticity of the raw materials as revealed by our analyses. However, this does not mean that reliable, durable products cannot be obtained with this material when it is fired at higher temperatures.

As regards to their colour, LB and PF fired samples show higher lightness (L*) values and, in most cases, higher chromaticity (a* and b*) values than the raw samples (Table 2). The increase in the L* value may be due to modification of the brick surface from a rough texture when raw, to a smoother one when fired, in which particles are more closely linked. Whereas, the increase in a* and b* may result from the transformation of Fe-hydroxides or poorly crystallized Fe-oxides dispersed in the clayey material into hematite and from the liberation of iron, as a result of the collapse of clay minerals, and its transformation into iron oxide on firing (Kreimeyer, 1987; Maniatis et al., 1980). Fired PF samples show the highest a* and b* values. More specifically, PF bricks show a* value comprised between 22.5 and 28.1 and b* between 25.1 and 30.6; in LB bricks a* ranges between 16.5 and 19.5 and b* is between 20.6 and 26.1 (Table 2). Both types of bricks can be described as "red-orange".

3.2.1. Mineralogy

At a temperature of 750 °C, the clay minerals can no longer be detected, except for the dehydroxyled illite/muscovite phase (Ill and Phy, Fig. 2 and Table 3). Although the concentrations are progressively lower as the firing temperature increases, it disappears at 1000 °C. This illite/muscovite depletion is accompanied by the formation of mullite ($Al_6Si_2O_{13}$) especially in LB samples, the concentration of which increases with temperature. This new silicate phase nucleates and grows on the remaining muscovite substrate during its breakdown (Rodriguez Navarro et al., 2003). In PF samples only, calcite concentrations begin to decrease at temperatures around 800 °C following the reaction: $CaCO_3 \rightarrow CaO + CO_2$ and disappear above 850 °C (Cal, Fig. 2 and Table 3). As far as feldspars are concerned, alkaline low-temperature phases (orthoclase and microcline) are transformed into a more stable sanidine at high temperatures, while anorthite is only formed in PF bricks. In addition to the anorthite, other mineral phases formed in PF samples at high temperatures included gehlenite ($Ca_2Al_2SiO_7$) and wollastonite ($CaSiO_3$). These calcium silicates were formed by the reaction of the calcium oxide produced by the decomposition of the calcite with the silicates distributed in the samples (Cultrone et al., 2001). Gehlenite forms at 850 °C but its concentration begins to decrease at 900 °C as wollastonite appears. At 1000 °C only wollastonite is detected (Fig. 2 and Table 3).

The presence of the vitreous phase was inferred by the increase in background noise in the PF and LB sample diffractograms, fired at 900 °C and 1000 °C. Vitrification is more pronounced in the samples from Porto Ferro than in those from Lago Baratz (V, Table 3).

3.2.2. Texture

Quartz is the most frequently detected of the minerals that characterize Porto Ferro ceramics. It can be detected as isolated crystals or as a constituent of metamorphic rock fragments, such as gneiss and quartzite, and is the main constituent of the temper (Fig. 4a). The larger fragments, ranging from 1 mm to 2 mm, are mainly angular to subrounded in shape and often have a mosaic texture and undulose extinction. Iron oxides are mostly small and red to brown-coloured. The muscovite is scattered throughout the matrix. We also observed fragments of carbonates with micritic texture and sometimes with reaction edges. The matrix of the samples fired at 750 °C and 800 °C is red-coloured and shows unidirectionally-oriented, elongated pores, which result from the pressure exerted on the raw material when it was placed in

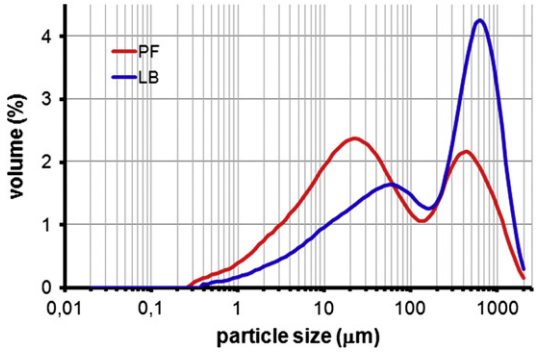

Fig. 3. Grain size distribution curves for Porto Ferro (PF) and Lago Baratz (LB) raw materials. Volume (in %) versus particle size (in μm).

Table 2
Brightness (L*) and chromaticity (a*, b*) values of Porto Ferro (PF) and Lago Baratz (LB) brick samples, unfired and fired at 750, 800, 850, 900 and 1000 °C.

Sample	L*	a*	b*
PF	46.61	12.53	15.33
PF750	58.01	24.03	26.64
PF800	55.44	23.18	25.08
PF850	51.31	22.54	24.27
PF900	52.48	24.72	26.64
PF1000	50.08	28.09	30.64
LB	50.41	9.23	13.46
LB750	53.98	17.38	21.13
LB800	54.60	17.93	21.80
LB850	53.31	17.68	22.03
LB900	55.64	16.54	20.60
LB1000	55.10	19.49	26.11

Table 3
XRD mineralogical analysis results of bricks of Porto Ferro (PF), and Lago Baratz (LB) fired at 750, 800, 850, 900 and 1000 °C. Qz = quartz; Phy = phyllosilicates (in general); Cal = calcite; Hem = hematite; Fsp = feldspars (in general); Mu = mullite; Gh = gehlenite; Wo = wollastonite; and V = vitreous phase. * is anorthite, ** is sanidine. Mineral symbols after Whitney and Evans (2010).

	Qz	Phy	Cal	Hem	Fsp	Mu	Gh	Wo	V
PF750	58	20	4	6	12				
PF800	58	19	2	6	15				
PF850	58	10	1	5	18		5		3
PF900	58	5		4	18*		4	5	6
PF1000	58			4	17*	3		8	10
LB750	65	17		3	15				
LB800	65	16		4	15				
LB850	65	13		5	15				2
LB900	65	6		5	16**	5			3
LB1000	65			5	17**	8			5

the mould. This also explains why the phyllosilicates are also oriented in the same direction. At 900 °C the matrix is darker and less birefringent (Fig. 4b), something which is accentuated at 1000 °C, indicating that the brick is gradually vitrified (Fig. 4c). This confirms the XRD results on melt content described in the previous section. At this temperature phyllosilicate remains can be observed under the microscope. These may have been transformed into mullite, as suggested by XRD analysis, although these crystals are too small to be detected using POM. The spaces once filled by calcite crystals are now pores.

Quartz is also the most frequently occurring of the minerals that characterize the ceramics from the Lago Baratz. It has undulose extinction and irregular morphology and is found either as isolated crystals or as fragments of metamorphic rocks such as phyllites, quartzites, gneisses and micaschists, and is the main part of the temper (Fig. 4d). If we compare Fig. 4c and d, it is clear that the temper content is greater and more abundant in LB than in PF. Muscovite has a laminar habit and,

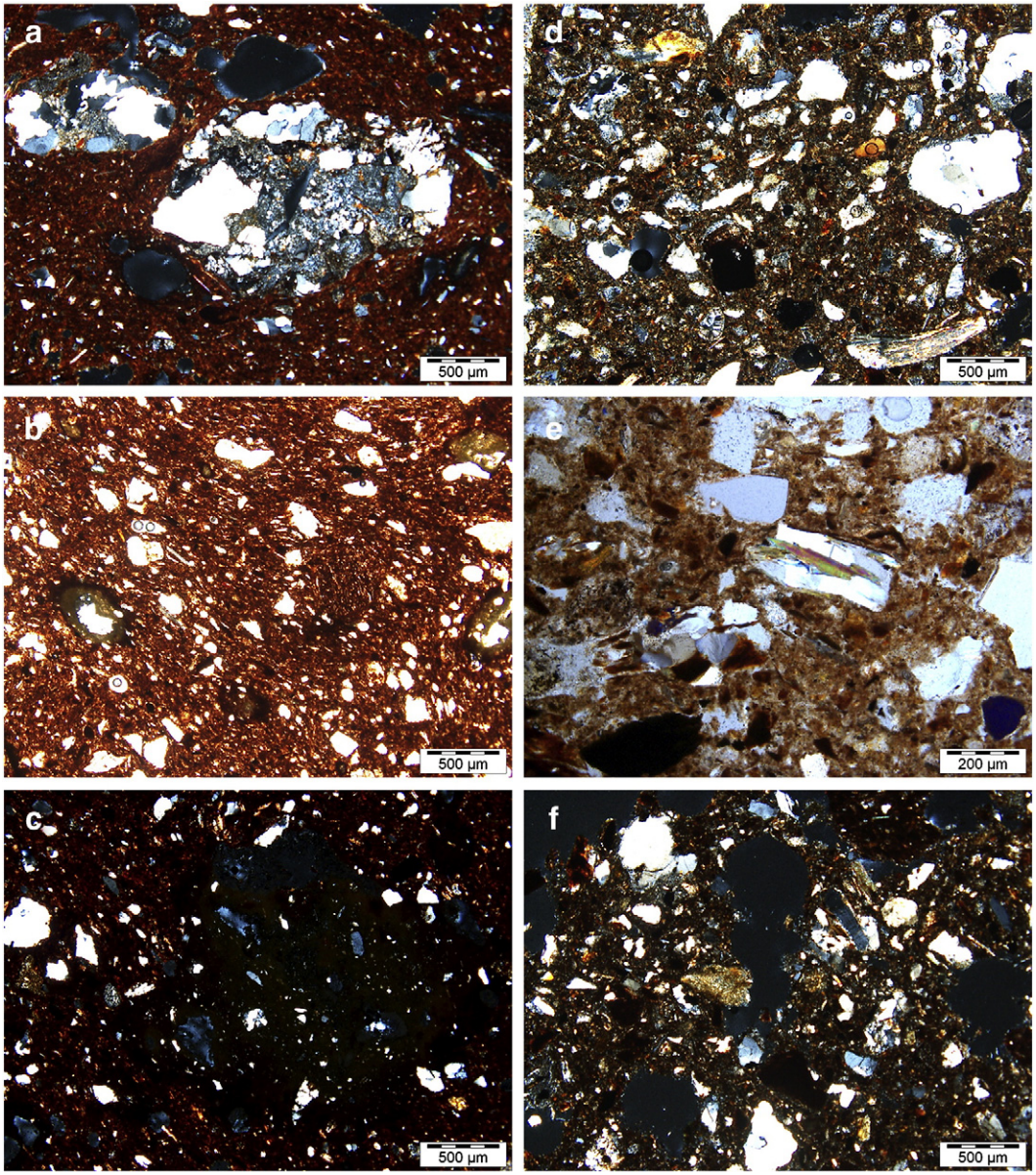

Fig. 4. Optical microscopy images of: a) gneiss fragments in PF750 sample (cross polars); b) aspect of the red matrix in PF900 sample in which the orientation of pores and phyllosilicates is visible (plane light); c) low birefringence of PF1000 sample (cross polars); d) general view of the matrix of LB750 (cross polars). Notice the higher temper content compared to PF samples; e) detail of LB900 sample in which the typical interference colours of muscovite crystals are still visible (cross polars); and f) general view of LB1000 characterized by a decrease in matrix birefringence (cross polars).

in some cases, folds could be observed in metamorphic fragments. However, the orientation of phyllosilicates is less pronounced than in PF bricks, because the higher amount of coarser particles "disturbs" the orientation of laminar minerals (Delbrouck et al, 1993). At 900 °C the matrix of this group of bricks is more birefringent than PF900, and the phyllosilicates show higher interference colours (Fig. 4e). At 1000 °C the degree of vitrification increases, as evidenced by the decrease of matrix birefringence (Fig. 4f), although it does not reach the same low level as PF1000.

In order to amplify XRD and POM findings about the mineralogical and textural changes in PF and LB bricks, the lowest (750 °C) and the highest fired samples (1000 °C) were observed under FESEM. Firing at 750 °C does not induce evident textural changes. Only phyllosilicates exfoliate along their basal planes due to dehydroxylation. No signs of vitrification are visible at this temperature (Fig. 5a). In PF bricks, calcite grains with micritic texture are still present confirming the results of the XRD analysis (Fig. 2 and Table 3). They are characterized by micrometric holes, i.e. the pre-existing pores in the raw material whose shape is delimited by the boundaries of carbonate crystals, and also the nanometric black spots inside the crystals, which presumably are new empty spaces generated by the incipient decomposition of carbonate and the release of CO_2 (Fig. 5b). On this question, Rodriguez Navarro et al.

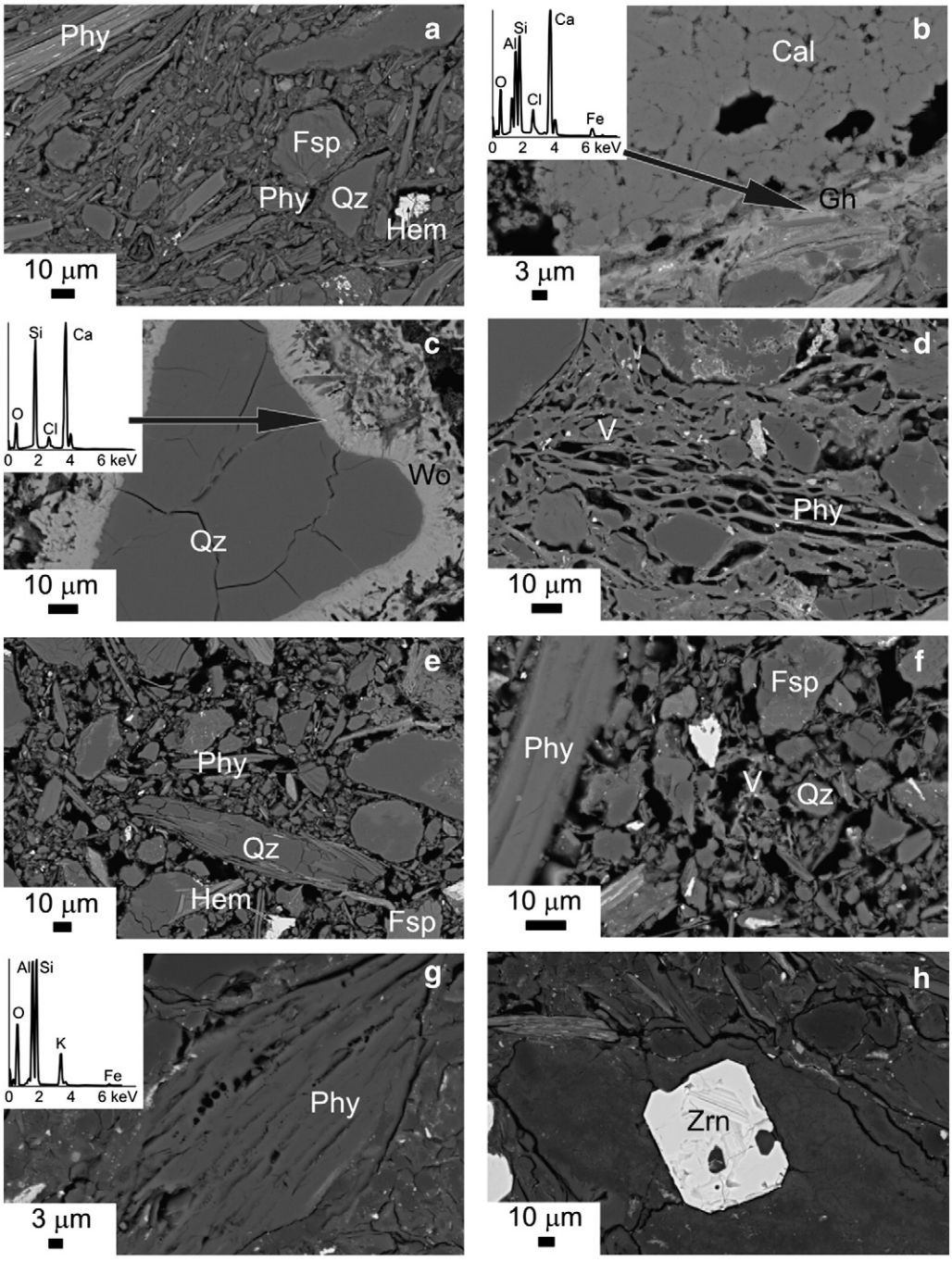

Fig. 5. FESEM images and EDX analyses of Porto Ferro and Lago Baratz bricks fired at 750 and 1000 °C: a) general view of PF750 sample; b) detailed image of a calcite grain in PF750 sample showing a white outer reaction rim of gehlenite; c) quartz grain with smoothed edges surrounded by fibrous wollastonite crystals in PF1000 sample; d) development of secondary porosity in PF1000 sample due to the high firing temperature; e) general aspect of LB750 sample; f) texture of LB brick fired at 1000 °C; g) development of bloating pores in a phyllosilicate of LB brick fired at 1000 °C and presence of small fissures around grains; and h) idiomorphic zircon crystal in LB1000 sample. Legend: Qz = quartz; Phy = phyllosilicate (illite); Cal = calcite; Hem = hematite; Fsp = feldspars; Gh = gehlenite; Wo = wollastonite; Zrn = zircon; and V = vitreous phase. Mineral symbols after Whitney and Evans (2010).

(2009) observed that the thermal decomposition of calcite starts early at around 600 °C, is completed at about 850 °C and is accompanied by the development of a nanoporosity inside the crystals. Another important finding is that at 750 °C a reaction along the calcite/matrix interface with the development of a thin (less than 10 μm) ring of gehlenite (Fig. 5b and EDX analysis) is observed. The presence of this silicate phase in ceramics, albeit in very low amounts (which explains why it was not detected by XRD), indicates that it is formed at a lower temperature than those generally reported in the bibliography (more than 800 °C according to Peters and Iberg, 1978; Grapes, 2006; Maritan et al., 2006; Trinidade et al., 2009; Rathossi and Pontikes, 2010).

At 1000 °C no more calcite is visible and where it had been present there are now pores with light grey colours along the edges where the reaction with the silicate matrix took place. Gehlenite has been replaced by wollastonite, as evidenced by the thick rings of $CaSiO_3$ with a fibrous shape that envelop the quartz grains which, because of the reaction become rounded (Fig. 5c and EDX analysis).

Wollastonite may be formed either by the decomposition of gehlenite, which in this case also leads to the crystallisation of anorthite (Peters and Iberg, 1978) (1), or directly from CaO (2) as follows:

$$Ca_2Al_2SiO_7 + SiO_2 \rightarrow CaSiO_3 + CaAl_2Si_2O_8 \quad (1)$$

$$CaO + SiO_2 \rightarrow CaSiO_3 \quad (2)$$

The texture of PF bricks changes radically: grains are well joined to each other by a totally vitrified matrix; pores augment in size and change from angular to ellipsoidal in shape. Moreover, a secondary porosity (Cairo et al., 2001) develops in the matrix or within the minerals which is rounded in shape. The most evident of these pores are the bubbles that develop inside the phyllosilicates (Fig. 5d), which have a morphology consistent with the "cellular structure" described by Tite and Maniatis (1975).

The texture of LB bricks is clearly different from the other group. In fact, at 750 °C it seems that grains are not well joined to the matrix suggesting a partial weakness of the material (Fig. 5e). A higher amount of empty spaces can be seen and the amount of finer fraction is visibly lower than in PF bricks. The main textural change at this temperature is again the dehydroxylation of phyllosilicates (Fig. 5e). At 1000 °C, even if the porosity and pore size seem to have suffered no substantial changes, the particles are welded to each other. A detailed observation confirms that vitrification has been reached since the particles are now joined together by melt (Fig. 5f). Two types of pores can be seen: a) small fissures due to shrinkage at grain boundaries, and b) fine bloating pores in the glass matrix or inside laminar minerals (Fig. 5g and EDX analysis). While this second type of pore is common to both groups of bricks, the presence of fissures at the grain boundaries is characteristic of LB and has been explained by Kilikoglou et al. (1998) as the result of the shrinkage of clay platelets when drying and, above all, during firing when quartz α expands at 573 °C to transform into polymorph β while the matrix shrinks in size at temperatures over 800 °C.

With FESEM mullite crystals were not observed in either PF or LB bricks because they are too small to be detected using this technique. Mullite develops during illite/muscovite breakdown (Brearley and Rubie, 1990; Rodriguez Navarro et al., 2003), but only a partial enrichment in Fe (presumably hematite) along some phyllosilicate layers is detected. In addition to hematite, zircon (Fig. 5h), rutile and ilmenite were identified based on EDX analysis. These grains ranged from 1–2 μm to 20–30 μm in size and were not detected in XRD.

3.2.3. Hydric tests

Hydric properties help us to understand the behaviour of materials when in contact with fluids (especially water), i.e. how fluids are absorbed and evaporate. The degree of intergranular union, the presence of anisotropy and the pore opening radius are all factors affecting the movement of fluids inside a material (Esbert et al., 1991) and in this study may provide useful information on the quality of the two groups of bricks.

It is important to point out that hydric tests were not performed on the LB samples fired at 750 and 800 °C because they crumbled when submerged in water. Such behaviour indicates a low degree of cohesion between the matrix and the temper. On this question, the analysis of the raw material previously described showed its high content in coarse fraction and the poor union between the particles of fired bricks below 850 °C.

The real density values (ρ_{sk}, Table 4) are similar for both groups of bricks especially around 900 °C (ρ_{sk} ranges between 2511 and 2590 kg/m^3 in PF and between 2526 and 2632 kg/m^3 in LB) and are typical for this type of material. The open porosity values (p_o, Table 4) measured in PF and LB samples are similar to those for bricks from historical buildings (Fernandes et al., 2010) and are always higher than industrially extruded bricks (Delbrouck et al., 1993). During the free absorption test, the bricks that retained the least amount of water at the end of the analysis were the PF samples fired at 1000 °C (Fig. 6 and value of A_b in Table 4). As the firing temperature increases, the water absorption capacity gradually decreases, together with the open porosity value (p_o, Table 4) and the samples take slightly longer to dry (Di, Table 4). This behaviour is due to the progressive vitrification of the Porto Ferro ceramics, which reduces the connectivity between pores (Cultrone et al., 2004). However, the reduction in porosity and water absorption is low and there is only one abrupt fall when the temperature passes 900 °C (see also the decrease in saturation coefficient, S, in Table 4). This indicates a development in the vitreous phase at 1000 °C shown in Table 3.

As one might expect, LB bricks behave differently from PF bricks because the differences in the granulometry and mineralogy of the raw materials are due to: (1) PF is a silty sand and therefore has a higher plasticity than LB which is a sand; and (2) PF has calcite among its mineral components whereas LB has no carbonates and is richer in quartz and kaolinite. These factors have a significant influence on the hydric behaviour of the fired products (Freyburg and Schwarz, 2007). In LB, the changes in the hydric values as temperature increased were less marked than in PF and sometimes even moved in the opposite direction. The p_o value in LB increased while in PF it fell because of a combination of two factors: the presence of a coarser texture and the lower degree of vitrification attained (see Fig. 5). As regards to the first factor, it has already been proved that the addition of temper (thereby increasing the coarser fractions in a clayey material) reduces differences in the hydric behaviour of bricks fired at different temperatures (Cultrone et al., 2005a). In fact, fissures develop at grain boundaries and an extensive network amongst the pores is visible (Kilikoglou et al., 1998) which

Table 4
Hydric parameters of the ceramics of Porto Ferro (PF) and Lago Baratz (LB) fired at 750, 800, 850, 900 and 1000 °C. Legend: A_b = free water absorption (%); Af = forced water absorption (%); Di = drying index; S = saturation coefficient (%); p_o = open porosity (%); ρ_b = apparent density (kg m^{-3}); and ρ_{sk} = real (skeletal) density (kg m^{-3}). The standard deviation of three measurements is shown in brackets.

	PF750	PF800	PF850	PF900	PF1000	LB850	LB900	LB1000
A_b	20.07 (0.16)	19.68 (0.18)	19.42 (0.16)	19.13 (0.33)	13.36 (0.40)	15.72 (0.42)	16.21 (1.53)	15.82 (0.48)
A_f	20.56 (0.07)	20.20 (0.19)	19.89 (0.21)	19.41 (0.54)	13.57 (0.49)	16.21 (0.66)	16.37 (1.58)	16.25 (0.07)
Di	895 (0)	897 (0.01)	901 (0)	904 (0.01)	906 (0)	909 (0)	907 (0.01)	905 (0)
S	82.56 (0.70)	82.67 (0.75)	81.30 (1.14)	82.25 (1.28)	68.19 (1.96)	79.33 (2.31)	81.26 (5.22)	78.38 (0.62)
p_o	34.63 (0.51)	34.26 (0.38)	33.63 (0.17)	33.05 (0.64)	25.31 (0.66)	29.05 (1.06)	29.82 (2.59)	29.96 (0.07)
ρ_b	1653 (0.02)	1662 (0.01)	1684 (0.01)	1692 (0.01)	1698 (0.02)	1792 (0.01)	1822 (0.02)	1844 (0)
ρ_{sk}	2511 (0.05)	2536 (0.02)	2577 (0.01)	2584 (0)	2590 (0.01)	2526 (0.03)	2597 (0.06)	2632 (0)

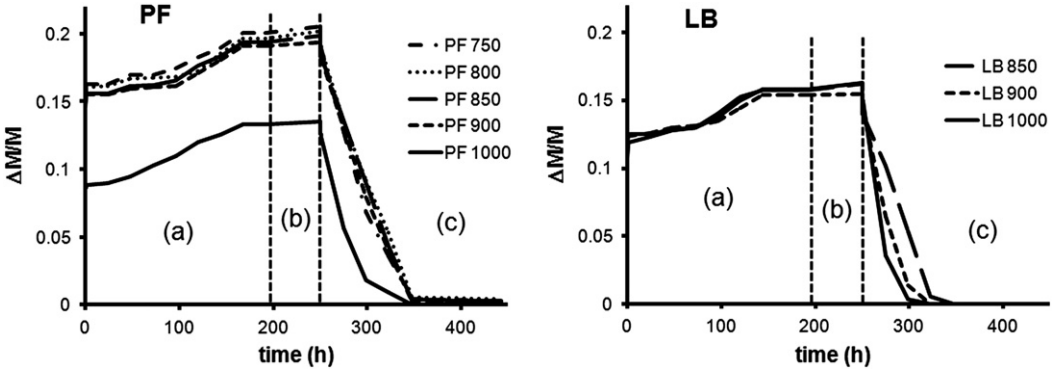

Fig. 6. Free water absorption (a), forced saturation (b) and drying (c) of bricks from Porto Ferro (PF) and Lago Baratz (LB) fired at 750, 800, 850, 900 and 1000 °C. Weight variation (ΔM/M) over time (in hours).

maintains almost unchanged hydric values. As for the second factor, during vitrification the texture of bricks changes considerably (and their pore system too), increasing their compressive strength and reducing their water absorption (Manoharan et al., 2011). We have observed (Table 3 and Fig. 5) however, that this phenomenon is less marked in LB. The high percentage of coarse grains and the low vitrification level results in uniform bricks from the hydric point of view, as they are characterized by similar absorption (A_b) and drying values (Di). This homogeneous hydric behaviour over a wide temperature range could be of practical use in the production process to ensure that similar pieces are obtained even if the firing temperature cannot be controlled correctly and fluctuations occur in the firing range between 850 and 1000 °C.

3.2.4. Ultrasound

V_{P2} and V_{P3} velocity values are similar in all bricks, and, in any case, higher than the V_{P1} value, because the latter was measured along the direction of the pressure exerted on the clayey mass when it was placed in the wooden mould. The clay minerals are therefore arranged perpendicularly to the direction of the propagation of the ultrasonic waves.

Velocity increases with temperature in both PF and LB samples (Table 5). The average velocity increase is more pronounced in the Lago Baratz ceramics (+58.6%) than in the samples from Porto Ferro (+28.7%). However, the V_P values measured in LB samples are lower than PF, proving that the samples are not very compact (remember that LB materials become brittle when fired at low temperatures) and do not reach the same vitrification level as mentioned earlier. Their quality improves (and the V_P increases) as the firing temperature increases, but not enough to reach the level of quality shown by the Porto Ferro ceramics. Firing temperatures significantly higher than 1000 °C would be necessary to achieve velocities similar to those observed in the Porto Ferro samples. The highest V_P values belonged to PF900 ($\bar{V}_P$ = 1608 m/s) and PF1000 ($\bar{V}_P$ = 1685 m/s) and are similar to those measured in historical buildings (Cultrone et al. 2005b; Fort et al., 2007). However, as might be expected, these values were lower than those for a less porous extruded brick which reaches a V_P of, at least, 2300 m/s (Binda and Baronio, 1984).

Table 5
Propagation velocity of ultrasonic waves (V_P in m/s) and values of total and relative anisotropy (ΔM and Δm in %) of Porto Ferro (PF) and Lago Baratz (LB) bricks, fired at 750, 800, 850, 900 and 1000 °C. The standard deviation of three measurements is shown in brackets.

Sample	V_{P1}	V_{P2}	V_{P3}	ΔM	Δm
PF750	1122 (54)	1480 (60)	1325 (49)	19.99 (3.5)	11.06 (0.8)
PF800	1250 (59)	1581 (141)	1398 (84)	15.96 (2.6)	12.15 (3.3)
PF850	1232 (66)	1688 (31)	1475 (51)	22.11 (3.6)	13.53 (2.0)
PF900	1475 (65)	1754 (75)	1594 (52)	11.89 (3.6)	9.51 (2.3)
PF1000	1572 (75)	1805 (170)	1677 (144)	9.50 (3.7)	7.29 (0.9)
LB850	569 (60)	660 (48)	622 (45)	10.97 (3.6)	5.88 (1.0)
LB900	691 (99)	766 (26)	738 (50)	8.14 (0.1)	3.64 (0.5)
LB1000	941 (87)	1014 (24)	990 (50)	6.09 (0.7)	2.41 (0.4)

The anisotropy values (ΔM and Δm, Table 5) are affected by the fact that the samples were prepared by hand, and vary according to the pressure exerted on the clayey mass in the wooden mould. In general, the anisotropy decreases as the temperature increases because the degree of vitrification increases and the pores acquire a rounder shape (Papargyris et al., 2001). Notice how the anisotropy is noticeably lower in LB bricks than in PF bricks confirming the "disturb" effect of coarse grains on the orientation of clay minerals.

3.2.5. Accelerated ageing test

All samples were damaged and suffered loss of material. Damage always appeared first at the edges and corners and then spread across the surface and inside the sample. Overall, the PF and LB samples behaved in similar ways. Sodium sulphate crystallisation occurred most frequently in Porto Ferro samples fired at the lowest temperature (PF750, Fig. 7), as they immediately began to gain weight due to the presence of salts in the pore system. Their weight increased again in the 3rd and 4th cycles due to cracking processes which favoured the intrusion of more salt, completely breaking the sample in the 5th cycle. According to Steiger and Asmussen (2008), the damage of samples occurs mainly during the wetting phase when the decahydrate sodium sulphate (mirabilite) grows from the highly supersaturated solution originating from the dissolution of anhydrous sodium sulphate (thenardite). Greater levels of resistance to deterioration increased in line with the firing temperature. In fact, PF800, PF850 and PF900 samples behaved better than those of PF750 because the higher the firing temperature, the higher the compactness of the bricks (see V_P values, Table 5). In any case, from the 3rd–4th cycle onwards, these samples also began to lose fragments due to the pressure exerted by the salts in the pores and the fissures. The PF1000 samples were the only ones to last the full ten cycles without breaking, and also showed the smallest weight increase because of their extensive vitrification. In fact, when bricks reach vitrification they become more compact and less saline solution can intrude due to changes in the pore system (Binda and Baronio, 1984). In the LB group the situation was similar: the samples fired at 850 and 900 °C registered a weight increase just after the 1st cycle and then underwent a slow but constant decay, which worsened from the 6th cycle onwards (Fig. 7). The samples fired at 1000 °C behaved similarly to PF1000 with only a small weight increase.

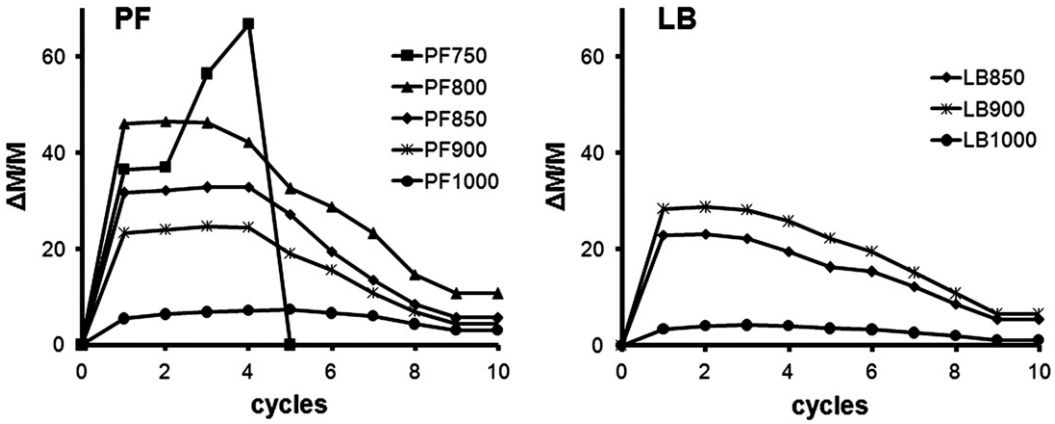

Fig. 7. Weight variation (ΔM/M) in samples from Porto Ferro (PF) and Lago Baratz (LB) fired at 750, 800, 850, 900 and 1000 °C and subjected to ten salt crystallisation cycles.

After the test, the samples were washed several times in distilled water to remove residual salts and were weighed in order to calculate the real percentage of weight loss (Table 6). In both groups, weight loss was greater in the samples fired at lower temperatures and decreased as the firing temperature increased, showing an abrupt descent at 1000 °C, which is logical since these bricks showed the highest levels of vitrification. However, it is interesting to note that in this aggressive test PF and LB fired at the highest temperature acted in almost the same ways, although we observed that the bricks from Lago Baratz did not reach the same vitrification level as those from Porto Ferro. The coalescence between particles observed in LB bricks fired at 1000 °C (Fig. 5f) was enough to counteract the damaging effect of salt.

4. Conclusions

This study compared two groups of bricks manufactured using raw materials sampled in the northwest of Sardinia (Italy). According to the Shepard nomenclature the raw material from the Lago Baratz is a sand, and it is brown and rich in quartz and phyllosilicates. It is similar to the clay from Porto Ferro both in terms of colour and mineral content, but the latter also contains calcite and has a finer, more plastic granulometry as it is a silty sand. When fired, both brick groups are red-orange coloured and undergo significant mineralogical and textural changes. These affect the decomposition of clay minerals and carbonates and the formation of new silicate phases, while the matrix becomes less birefringent due to vitrification. Gehlenite appears at just 750 °C and is replaced at higher temperatures by fibrous wollastonite. At 900 and 1000 °C mullite was also detected. This mineral was probably formed due to the decomposition of muscovite-type phyllosilicates. The samples from Lago Baratz fired at 750 and 800 °C could not be studied from the physical point of view due to the low degree of cohesion between the matrix and the coarser fraction and the addition of a finer granulometry with higher plasticity may be advisable.

The ceramics prepared using the clayey material from Porto Ferro showed the most balanced results in terms of physical parameters and durability. More specifically, hydric tests show that Porto Ferro is the best raw material for producing high quality bricks, and the higher the firing temperature, the better the quality of the product. However, the possible use of the raw material from Lago Baratz in brick production cannot be discarded because these bricks show similar hydric behaviour over a wide range of firing temperatures (850 to 1000 °C), which means that bricks with similar physical properties can be produced even if the temperature of the oven fluctuates.

Ultrasound indirectly confirmed the higher vitrification reached by the bricks from Porto Ferro as they were found to be more compact. A higher firing temperature, and therefore greater expense, is required to give the bricks from the Lago Baratz the same degree of compactness. However, the degree of vitrification reached by these bricks is enough to ensure samples of the same good quality as those from Porto Ferro, as the accelerated ageing test has demonstrated.

This work has proved a useful means of evaluating the quality of two raw materials for their potential use in brick production and may encourage the development of this activity in northwest Sardinia.

Table 6
Weight loss (%) of Porto Ferro (PF) and Lago Baratz (LB) samples fired at 750, 800, 850, 900 and 1000 °C after the salt crystallisation cycles. The standard deviation of three measurements is shown in brackets.

Sample	750 °C	800 °C	850 °C	900 °C	1000 °C
PF	100 (0)	47.86 (8.4)	34.62 (2.6)	28.46 (3.4)	5.79 (1.7)
LB			36.04 (12.9)	45.11 (13.4)	4.33 (0.2)

Acknowledgements

This study was financially supported by the Research Group RNM179 of the Junta de Andalucía, by the Research Project P09-RNM-4905 and by the ICON-CICOP Institute of Granada. We are grateful to Julia Castro for her collaboration in the estimation of the Atterberg limits, to Nigel Walkington for his assistance in translating the original text and to Jeanne Percival and two anonymous referees for their in-depth review of the manuscript.

References

Alba, E., 2009. Métodos de análisis territorial aplicados a la ocupación de la zona de Alghero (Cerdeña, Italia) durante la Edad del Bronce. (Phd Thesis) Universidad de Granada.
Annis, M.B., 1985. Resistance and change: pottery manufacture in Sardinia. World Archaeol. 17, 240–255.
ASTM D 2845-08, 2008. Standard test method for laboratory determination of pulse velocities and ultrasonic elastic constants of rocks. ASTM International Standards Worldwide, Pennsylvania.
ASTM D 4318-10, 2010. Standard test methods for liquid limit, plastic limit and plasticity index of soils. ASTM International Standards Worldwide, Pennsylvania.
Bain, J.A., Highley, D.E., 1979. Regional appraisal of clay resources. A challenge to the clay mineralogist. Proceedings of the VI International Clay Conference 1978, under the Auspices of AIPEA, Oxford. Developments in Sedimentology, 27, pp. 437–446.
Bajare, D., Svinka, V., 2000. Restoration of the historical brick masonry. In: Fassina, V. (Ed.), Proceedings of the 9th International Congress on Deterioration and Conservation of Stone. Venice, pp. 3–11.
Binda, L., Baronio, G., 1984. Measurement of the resistance to deterioration of old and new bricks by means of accelerated aging tests. Durab. Build. Mater. 2, 139–154.
Brearley, A.J., Rubie, D.C., 1990. Effects of H_2O on the disequilibrium breakdown of muscovite + quartz. J. Petrol. 31, 925–956.
Cairo, A., Messiga, B., Riccardi, M.P., 2001. Technological features of the "Cotto Variegato": a petrological approach. J. Cult. Herit. 2, 133–142.
Carboni, R., Cicu, E., Cruccas, E., Corrias, F., 2012. Turris Lilibonis, terme Pallottino: nuovi scavi e ricerche. L'Africa Romana XIX, 2577–2595.
Carmignani, L., 2001. Carta Geologica della Sardegna. Servizio Geologico Nazionale, Regione Autonoma della Sardegna. Assessorato all'Industria. A cura del Comitato

per il Coordinamento della Cartografia Geologica e Geotematica della Sardegna, scala 1:200000.
Cassinis, G., Cortesogno, L., Gaggero, L., Ronchi, A., Valloni, R., 1996. Stratigraphic and petrographic investigations into the Permian-Triassic continental sequences of Nurra (NW Sardinia). Cuad. Geol. Iber. 21, 149–169.
Chen, G., Wang, J., 1998. The preparation of marine geological certified reference materials—polymetallic nodule GSPN-1 and marine sediment GSMS-1 from the Central Pacific Ocean. Geostand. Geoanal. Res. 22, 119–125.
Cita Sironi, M.B., Abbate, E., Balini, M., Conti, M.A., Falorni, P., Germani, D., Groppelli, G., Manetti, P., Petti, F.M., 2006. Carta Geologica d'Italia 1:50.000. Catalogo delle formazioni – Unità Tradizionali. Quaderni serie III, Volume 7, Fascicolo VII, APAT, Rome.
Colombi, R., 2010. Indigenous settlements and Punic presence in Roman republican Northern Sardinia. Bollettino di Archeologia on-line, Volume Speciale, 13-24.
Cultrone, G., Rodriguez Navarro, C., Sebastián Pardo, E., Cazalla, O., de la Torre, M.J., 2001. Carbonate and silicate phase reactions during ceramic firing. Eur. J. Mineral. 13, 621–634.
Cultrone, G., Sebastián, E., Elert, K., de la Torre, M.J., Cazalla, O., Rodríguez Navarro, C., 2004. Influence of mineralogy and firing temperature on porosity of bricks. J. Eur. Ceram. Soc. 24, 547–564.
Cultrone, G., Sebastián, E., de la Torre, M.J., 2005a. Mineralogical and physical behaviour of solid bricks with additives. Constr. Build. Mater. 19, 39–48.
Cultrone, G., Sidraba, I., Sebastián, E., 2005b. Mineralogical and physical characterization of the bricks used in the construction of the "Triangul Bastion", Riga (Latvia). Appl. Clay Sci. 28, 297–308.
de Buergo, Álvarez, Ballester, M., González Limón, T., 1994. Restauración de edificios monumentales. CEDEX, Madrid.
de Canales, González, Cerisola, F., Serrano Pichardo, L., Llompart Gómez, J., 2006. The precolonial Phoenician emporium of Huelva ca. 900–770 BC. Babesch 81, 13–29.
De Rosa, B., 2010. Sant'Imbenia (Alghero, SS). Il contributo dell'archeometria nella ricostruzione della storia e delle attività dell'abitato nuragico. Unpublished PhD Thesis, University of Sassari (Italy).
De Rosa, B., Cultrone, G., Rendeli, M., 2012. Archaeometric reconstruction of Nuragic ceramics from Sant'Imbenia (Sardinia, Italy). Technological evolution of production process. Periodico di Mineralogia 81, 313–332.
Delbrouck, O., Janssen, J., Ottenburgs, R., Van Oyen, P., Viaene, W., 1993. Evolution of porosity in extruded stoneware as a function of firing temperature. Appl. Clay Sci. 7, 187–192.
Dondi, M., 2011. Argille per laterizi in Italia: giacimenti e tendenze nel periodo 1960–2010. Aracne Editrice, Rome.
Dondi, M., Fabbri, B., 2001. Le materie prime dell'industria ceramica italiana. In: Jiménez Millán, J. (Ed.), Materias primas y métodos de producción de materiales cerámicos, pp. 41–64. Baeza (Jaén).
Dondi, M., Fabbri, B., Sistu, G., 1995. Le argille da laterizi della Sardegna: caratteristiche composizionali e influenza sulle proprietà dei prodotti. Rendiconti Seminario Facoltà Scienze Università Cagliari 65, 219–238.
Dondi, M., Ercolani, G., Fabbri, B., Guarini, G., Marsigli, M., Mingazzini, C., 1999a. Major deposits of brick clays in Italy. Part 1: Geology and Composition. Tile & Brick International, 15, pp. 230–237.
Dondi, M., Ercolani, G., Fabbri, B., Guarini, G., Marsigli, M., Mingazzini, C., 1999b. Major deposits of brick clays in Italy. Part 2: Technological Properties and Uses. Tile & Brick International, 15, pp. 360–370.
Elert, K., Cultrone, G., Rodriguez Navarro, C., Sebastián Pardo, E., 2003. Durability of bricks used in the conservation of historic buildings. Influence of composition and microstructure. J. Cult. Herit. 4, 91–99.
EN 12370, 2001. Metodi di prova per pietre naturali. Determinazione della resistenza alla cristallizzazione dei sali. CNR-ICR, Rome, Italy.
EN 13755, 2008. Metodi di prova per pietre naturali. Determinazione dell'assorbimento d'acqua a pressione atmosferica. CNR-ICR, Rome, Italy.
Esbert, R.M., Montoto, M., Ordaz, J., 1991. La piedra como material de construcción: durabilidad, deterioro y conservación. Mater. Constr. 41, 61–71.
Esbert, R.M., Ordaz, J., Alonso, F.J., Montoto, M., González Limón, T., de Buergo, Álvarez, Ballester, M., 1997. Manual de diagnosis y tratamiento de materiales pétreos y cerámicos. Collegi d'Apparelladors i Arquitectes Tècnics de Barcelona, Barcelona.
Espinosa Marzal, R.M., Hamilton, A., McNall, M., Whitaker, K., Scherer, G.W., 2011. The chemomehanics of crystallization during rewetting of limestone impregnated with sodium sulfate. J. Mater. Res. 26, 1472–1481.
Fernandes, F.M., Lourenço, P.B., Castro, F., 2010. Ancient clay bricks: manufacture and properties. In: Bostenaru Dan, M., Přikryl, R., Török, Á. (Eds.), Materials, Technologies and Practice in Historic Heritage Structures. Springer, pp. 29–48.
Fort, R., Varas, M.J., Pérez-Monserrat, E., Luque, J., Álvarez de Buergo, M., Vázquez-Calvo, C., 2007. Los ladrillos del recinto amurallado de Talamanca de Jarama, Madrid: criterios para su diferenciación. Boletín de la Sociedad Española de Cerámica y Vidrio 46, 145–152.
Freyburg, S., Schwarz, A., 2007. Influence of the clay type on the pore structure of structural ceramics. J. Eur. Ceram. Soc. 27, 1727–1733.
Fundoni, G., 2009. Le relazioni tra la Sardegna e la Penisola Iberica nei primi secoli del I millennio a.C.: le testimonianze nuragiche nella Penisola Iberica. Anales de Arqueología Cordobesa 20, 11–34.
Grapes, R., 2006. Pyrometamorphism. Springer, Berlin.
Guydader, J., Denis, A., 1986. Propagation des ondes dans les roches anisotropes sous contrainte évaluation de la qualité des schistes ardoisiers. Bull. Eng. Geol. 33, 49–55.
Huertas, J., Huertas, F., Linares, J., 1991. Evaluación de las fases no cristalinas en cerámicas arqueológicas por DRX. Boletín de la Sociedad Española de Mineralogía 14, 71–78.
Khalfaoui, A., Hajjaji, M., 2010. Assessment of the ceramic suitability of a raw clay. Ceram. Silik. 54, 295–302.
Kilikoglou, V., Vekinis, G., Maniatis, Y., Day, P.M., 1998. Mechanical performance of quartz-tempered ceramics: part I, strength and toughness. Archaeometry 40, 261–279.
Kreimeyer, R., 1987. Some notes on the firing colour of clay bricks. Appl. Clay Sci. 2, 175–183.
Laird, R.T., Worcester, M., 1956. The inhibiting of lime blowing. Trans. Br. Ceram. Soc 55, 545–563.
Lassinantti Gualtieri, M., Gualtieri, A.F., Gagliardi, S., Ruffini, P., Ferrari, R., Hanuskova, M., 2010. Thermal conductivity of fired clays: effects of mineralogical and physical properties of raw materials. Appl. Clay Sci. 49, 269–275.
Ligas, P., Uras, I., Dondi, M., Marsigli, M., 1997. Kaolinitic materials from Romana (northwest Sardinia, Italy) and their ceramic properties. Appl. Clay Sci. 12, 145–163.
Maniatis, Y., Simopoulos, A., Kostikas, A., 1980. Moessbauer study of the effect of calcium content on iron oxide transformation in fired clays. J. Am. Ceram. Soc. 64, 263–269.
Manoharan, C., Sutharsan, P., Dhanapandian, S., Venkatachalapathy, R., Asanulla, R.M., 2011. Analysis of temperature effect on ceramic brick production from alluvial deposits, Tamilnadu, India. Appl. Clay Sci. 54, 20–25.
Maritan, L., Nodari, L., Mazzoli, C., Milano, A., Russo, U., 2006. Influence of firing conditions on ceramic products: experimental study on clay rich in organic matter. Appl. Clay Sci. 31, 1–15.
Martín Ramos, J.D., 2004. Using XPowder, a software package for powder X-ray diffraction analysis. Legal Deposit GR 1001/04.
Milanese, M., 2013. Alghero, archeologia di una città medievale. Carlo Delfino Editore, Sassari.
Mitchell, J.K., Soga, K., 2005. Fundamentals of soil behavior, 3rd ed. John Wiley & Sons, Inc., Hoboken, New Jersey.
Moravetti, A., 1992. Il complesso nuragico di Palmavera. Sardegna Archeologica. Guide e Itinerari 20. Carlo Delfino, Sassari.
Normal 29/88, 1988. Misura dell'indice di asciugamento (drying index). CNR-ICR, Rome, Italy.
Oggiano, G., Mameli, P., 2012. Tectonic and litho-stratigraphic controls on kaolin deposits within volcanic successions: insights from the Kaoliniferous DISTRICT of Northwestern Sardinia (Italy). Ore Geol. Rev. 48, 151–164.
Papargyris, A.D., Cooke, R.G., Papargyri, S.A., Botis, A.I., 2001. The acoustic behavior of bricks in relation to their mechanical behavior. Constr. Build. Mater. 15, 361–369.
Peters, T., Iberg, R., 1978. Mineralogical changes during firing of calcium-rich brick clays. Ceram. Bull. 57, 503–509.
Rathossi, C., Pontikes, Y., 2010. Effect of firing temperature and atmosphere on ceramics made of NW Peloponnese clay sediments: part II. Chemistry of pyrometamorphic minerals and comparison with ancient ceramics. J. Eur. Ceram. Soc. 30, 1853–1866.
RILEM, 1980. Recommended test to measure the deterioration of stone and to assess the effectiveness of treatment methods. Mater. Struct. 13, 175–253.
Rodriguez Navarro, C., Cultrone, G., Sanchez Navas, A., Sebastian, E., 2003. TEM study of mullite growth after muscovite breakdown. Am. Mineral. 88, 713–724.
Rodriguez Navarro, C., Ruiz Agudo, E., Luque, A., Rodriguez Navarro, A.B., Ortega Huertas, M., 2009. Thermal decomposition of calcite: mechanisms of formation and textural evolution of CaO nanocrystals. Am. Mineral. 94, 578–593.
Rovina, D., Fiori, M., 2013. Sassari. Archeologia urbana. Felici Editore, Sassari.
Sánchez, C.J., 2001. El procesado cerámico. In: Jiménez Millán, J. (Ed.), pp. 97–116 (Baeza (Jaén)).
Scott, V.D., Love, G., 1983. Quantitative Electron-probe Microanalysis. John Wiley & Sons, New York.
Shepard, F.P., 1954. Nomenclature based on sand–silt–clay ratios. J. Sediment. Petrol. 24, 151–158.
Singer, F., Singer, S.S., 1963. Industrial Ceramics. Chapman & Hall Ldt., London.
Steiger, M., Asmussen, S., 2008. Crystallization of sodium sulfate phases in porous materials: the phase diagram Na_2SO_4–H_2O and the generation of stress. Geochim. Cosmochim. Acta 72, 4291–4306.
Strazzera, B., Dondi, M., Marsigli, M., 1997. Composition and ceramic properties of tertiary clays from southern Sardinia (Italy). Appl. Clay Sci. 12, 247–266.
Tite, M.S., Maniatis, Y., 1975. Examination of ancient pottery using the scanning electron microscope. Nature 257, 122–123.
Trevelyan, F.C., Haslam, R.A., 2001. Musculoskeletal disorders in a handmade brick manufacturing plant. Int. J. Ind. Ergon. 27, 43–55.
Trinidade, M.J., Dias, M.I., Coroado, J., Rocha, F., 2009. Mineralogical transformations of calcareous rich clays with firing: a comparative study between calcite and dolomite rich clays from Algarve, Portugal. Appl. Clay Sci. 42, 345–355.
Warren, J., 1999. Conservation of brick. Butterworth Heinemann, Oxford.
Whitney, D.L., Evans, B.W., 2010. Abbreviations for names of rock-forming minerals. Am. Mineral. 95, 185–187.
Winkler, H.G.F., 1954. Bedeutung der Korngrössenverteilung und des mineralbestandes von tonen für die herstellung grobkeramischer erzeugnisse. Ber. Dtsch. Keram. Ges 31, 337–343.